Chinese Chemical Letters 33 (2022) 968–972

Contents lists available at ScienceDirect

Chinese Chemical Letters

journal homepage: www.elsevier.com/locate/cclet

Two-dimensional coordination polymer-based nanosensor for sensitive and reliable nucleic acids detection in living cells

Yuzhi Xu[a], Yanfei Zhang[c], Huihui Yang[c], Wen Yin[c], Leli Zeng[a], Shuo Fang[d], Si-Yang Liu[b,*], Zong Dai[b,*], Xiaoyong Zou[c], Yihang Pan[a,*]

[a] Precision Medicine Center, Scientific Research Center, The Seventh Affiliated Hospital, Sun Yat-sen University, Shenzhen 518107, China
[b] Key Laboratory of Sensing Technology and Biomedical Instrument of Guangdong Province, School of Biomedical Engineering, Sun Yat-sen University, Guangzhou 510006, China
[c] School of Chemistry, Sun Yat-sen University, Guangzhou 510275, China
[d] Department of Oncology, The Seventh Affiliated Hospital, Sun Yat-sen University, Shenzhen 518107, China

ARTICLE INFO

Article history:
Received 14 April 2021
Revised 6 June 2021
Accepted 15 July 2021
Available online 22 July 2021

Keywords:
Coordination polymers
Nanosheets
Fluorescence biosensor
Nucleic acids detection
Living cells

ABSTRACT

A reliable and sensitive strategy which can assess nucleic acid levels in living cells would be essential for fundamental research of biomedical applications. Some nanomaterial-based fluorescence biosensors recently developed for detecting nucleic acids, however, are often with expensive, complicated and time-consuming preparation process. Here, by using a facile bottom-up synthesis method, a two-dimensional (2D) coordination polymer (CP) nanosheet, [Cu(tz)] (Htz = 1,2,4-triazole), was successfully prepared after optimizing reaction conditions. These ultrathin CP nanosheets with thickness of 4.7 ± 1.1 nm could readily form nanosensors by assembly with DNA probes, which exhibited a low limit of detection (LOD) for p53 DNA fragment as 144 pmol/L. Furthermore, by integrating [Cu(tz)] nanosheets with hybridization chain reaction (HCR) probes, miR-21, one kind of microRNA upregulated in many cancer cells, can be sensitively detected with a LOD of 100 pmol/L and monitored in living cells, giving consistent results with those obtained by quantitative reverse-transcription polymerase chain reaction (qRT-PCR) analysis. Thus [Cu(tz)] nanosheets, which not only possess much better nucleic acids sensing performance than bulk cystals, but also exhibit nucleic acid delivery functions, could be used as a novel nanoplatform in biomedical imaging and sensing applications.

Nucleic acids, including DNA and RNA, play vital roles in many life activities, like cell division, development, apoptosis, *etc*. [1]. Reliable assessment of nucleic acids expression levels in living cells, although vastly important for providing an insight into disease progression and various cellular processes, is still a challenge [2]. Among all of the sensing methods, fluorescence method provides powerful tools to accurately detect and monitor nucleic acids in real time due to its high sensitivity and imaging resolution [3]. However, the majority of techniques require lysis or fixing of cells, and the exogenous bioprobes are not efficiently internalized by living cells. Thus, the development of intracellular sensor that possesses efficient cellular uptake and outstanding sensing performance is highly desired [4]. Recently, nanomaterial-based fluorescence nanosensors for the sensing of nucleic acids have attracted great attentions, which usually rely on fluorescence resonance energy transfer (FRET) *via* strong interaction between fluorophore and quencher [5,6]. Moreover, the good biocompatibility and cellular uptake of nanomaterials ensure the efficient and live-cell analysis of nucleic acids by these strategies [7].

With unique structures and large surface areas, two-dimensional (2D) nanomaterials, which involve graphene, graphitic carbon nitride, transition metal dichalcogenides (TMD), *etc*., have been intensively studied [8] and used as nanoplatforms for biomedical applications [9,10], including drug/gene delivery, photothermal/photodynamic therapy, and biosensing both *in vitro* and *in vivo* [11]. Although these 2D nanomaterials are able to detect nucleic acids by adsorbing fluorophore-labeled single-stranded DNA (ssDNA) probes to construct fluorescence nanosensors, their preparation procedures are usually complex and time-consuming, inspiring the investigation on other alternative and novel 2D nanomaterials for the same purpose.

Coordination polymers (CPs) are periodic structures of metal ions and ligands connected through coordination bonds, which possess a lot of promising features, such as diverse functions, tun-

* Corresponding authors.
E-mail addresses: liusiyang@mail.sysu.edu.cn (S.-Y. Liu), daizong@mail.sysu.edu.cn (Z. Dai), panyih@mail.sysu.edu.cn (Y. Pan).

https://doi.org/10.1016/j.cclet.2021.07.041
1001-8417/

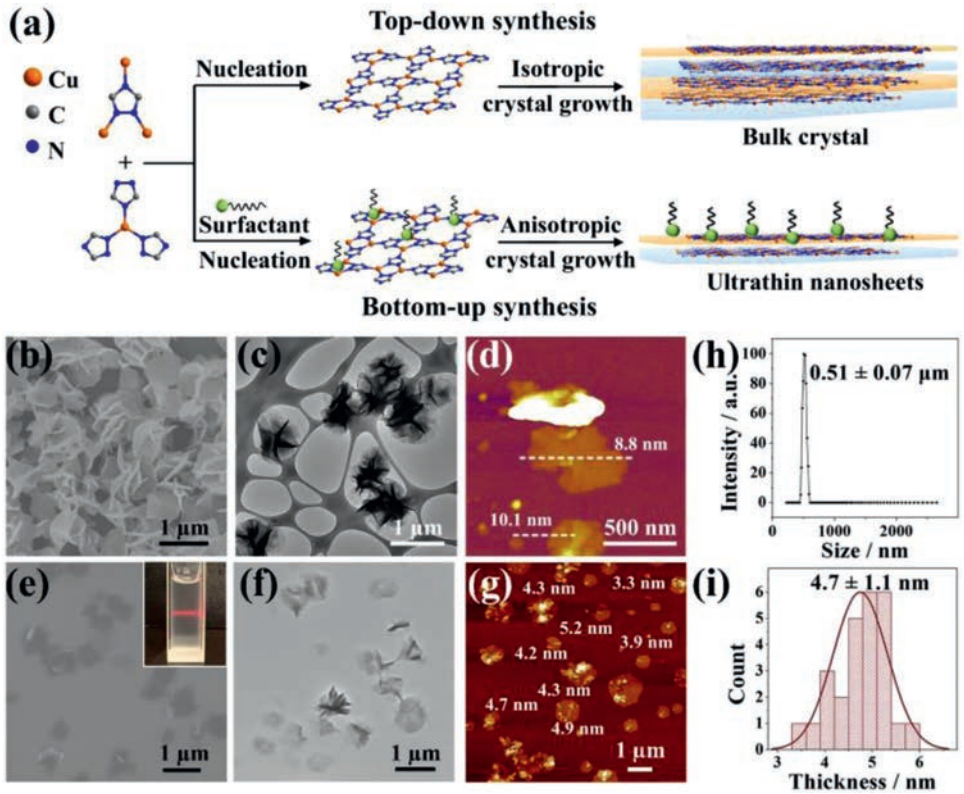

Fig. 1. (a) The top-down synthesis (top) and bottom-up synthesis (down) of CP. The flower-like [Cu(tz)] characterized by (b) SEM, (c) TEM and (d) AFM. The [Cu(tz)] nanosheets characterized by (e) SEM, (f) TEM, (g) AFM and (h) DLS. Inset in (e): Photograph of the Tyndall effect of the [Cu(tz)] nanosheet suspension in water. (i) The plot of thickness distribution of [Cu(tz)] nanosheets measured by AFM.

able structures, high surface area, good biocompatibility, and high loading capacity [12]. As a newly emerging class of 2D nanomaterials, 2D CP nanosheets have been successfully exfoliated from layered CP crystals [13]. The dramatically increased active sites and exposed surfaces of CP nanosheets comparing to their bulk forms make them superior candidates for catalysis, gas separation, and chemical sensing [14,15]. Compared with other 2D nanomaterials, the CP nanosheets have some advantages as a promising platform for biosensing including: (1) Higher level of structural tailorability by properly selecting metal ions and bridging ligands; (2) easy modification with different functional groups to specifically recognize target analytes; (3) intrinsic biodegradability after completing the task. Thus, the CP nanosheets have great potential to be used as a new kind of biosensing platform. However, the relatively strong interlayer interaction between the 2D coordination networks hinders the successful preparation of 2D CP nanosheets by exfoliation [16]. In comparison to the exfoliation (top-down) method, the bottom-up method, which is usually assisted with surfactant, is superior for preparing uniform and high-yield CP nanosheets [17].

Very recently, we proposed a bottom-up synthesis method of 2D CP nanosheets, [Cu(tz)] (Htz = 1,2,4-triazole), for cancer therapy [18]. In this paper, the synthesis method is further investigated to precisely control the size and morphology of the [Cu(tz)] nanosheets, which are applied for the study of DNA and microRNA (miRNA) sensing. Firstly, the widely reported top-down method, *i.e.*, sonication exfoliation method [19], was applied to prepare [Cu(tz)] nanosheets (Fig. 1a, top). The bulk crystals of [Cu(tz)] with millimeter sizes ($d \approx 1$ mm) were adopted as the raw material for sonication exfoliation, which were synthesized by the conventional solvothermal reaction using $Cu(NO_3)_2{\cdot}3H_2O$ and Htz as reactants and aqueous ammonia as solvent [20]. Though multiple combinations of sonication conditions and solvents were explored, the obtained samples possessed uneven size and large thickness (Fig. S1 in Supporting information). Therefore, bottom-up synthesis method was used to obtain the target ultrathin nanosheets of [Cu(tz)] (Fig. 1a, down). We found Cu_2O nanoparticle as an ideal and eco-friendly reactant for synthesizing Cu(I)-based CPs [21], which not only precluded the use of environment-hazardous solvents, but also reduced the particle size. By mixing Cu_2O nanoparticle ($d \approx 30–50$ nm) and Htz in aqueous phase containing polyvinylpyrrolidone (PVP, used as surfactant), and L-ascorbic acid (AA, used as deoxidant), under different conditions, different shaped [Cu(tz)] were obtained, which were then characterized by scanning electron microscopy (SEM), transmission electron microscopy (TEM) and atomic force microscopy (AFM). When the reaction temperature and metal concentration were relatively high ($T > 25$ °C, $C_{Cu_2O} > 0.1$ mg/mL), the obtained samples were flower-like with size around 1 μm and thickness around 10 nm (Figs. 1b–d). At lower reaction temperature of 10 °C and concentration of $C_{Cu_2O} = 0.1$ mg/mL, well-dispersed [Cu(tz)] nanosheets with less tendency for intercross growth were obtained (Figs. 1e–g). The SEM image showed a lateral size of 0.58 ± 0.15 μm for [Cu(tz)] nanosheets (Fig. 1e and Fig. S2 in Supporting information), which was in agreement with the dynamic light scattering (DLS) result of 0.51 ± 0.07 μm (Fig. 1h). The Tyndall effect observed in the aqueous solution of [Cu(tz)] nanosheets (inset in Fig. 1e) confirmed their aqueous dispersity. The low contrast in TEM image (Fig. 1f) and the thickness measured as 4.7 ± 1.1 nm by AFM (Figs. 1g and i) revealed the ultrathin nature of the nanosheets. Powder X-ray diffraction (PXRD) peaks of nanosheets were greatly broadened comparing to the flower-like and bulk [Cu(tz)] crystals (Fig. S3 in Supporting information), which can be ascribed to the thinner thickness [22]. The luminescence of [Cu(tz)] nanosheets

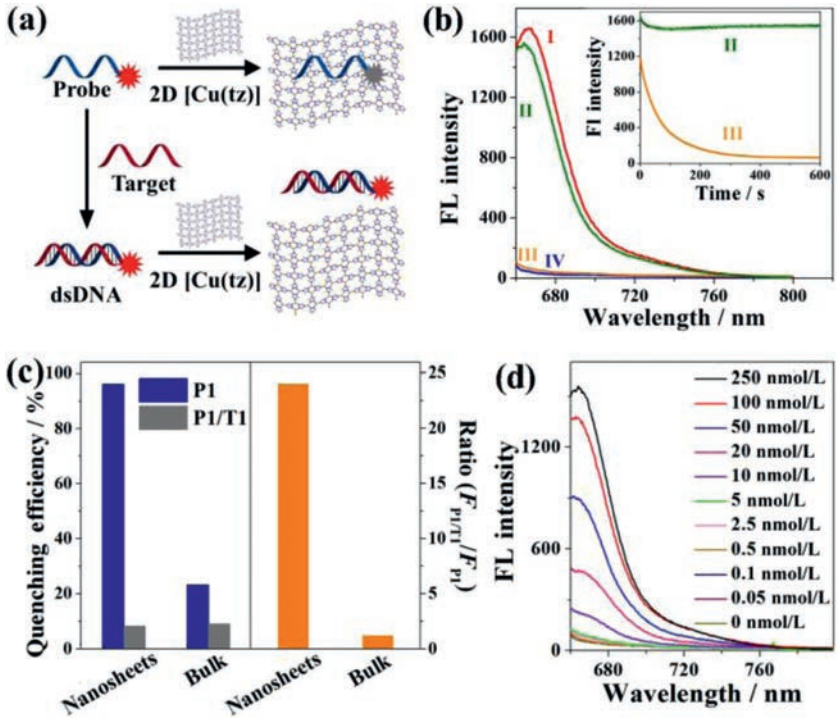

Fig. 2. (a) Schematic illustration of the fluorescence nanosensor for DNA detection based on [Cu(tz)] nanosheets. (b) Fluorescence spectra measured under various conditions: (I) 50 nmol/L of P1; (II) 50 nmol/L of P1 + 250 nmol/L of T1 + 100 μg/mL of nanosheet; (III) 50 nmol/L of P1 + 100 μg/mL of nanosheet; and (IV) 100 μg/mL of nanosheet. Inset: Kinetic change of fluorescence intensity at different conditions. (c) The quenching efficiency and ratio ($F_{P1/T1}/F_{P1}$) of nanosheets and bulk crystals of [Cu(tz)]. (d) Fluorescence spectra of P1 added with various concentrations of T1 and 100 μg/mL of nanosheet.

changed little after incubation in PBS for 8 h, suggesting a good stability of the nanosheets (Fig. S4 in Supporting information). The results confirmed that by controlling the conditions, ultrathin 2D [Cu(tz)] nanosheets with uniform size and good dispersity could be successfully obtained.

[Cu(tz)] nanosheets were used as a DNA sensing nanoplatform as a proof-of-concept demonstration (Fig. 2a). The conjugated π-electron system of triazolate ligand in [Cu(tz)] nanosheets allows for the binding of ssDNA probe *via* π-π stacking between the aromatic nucleobases of ssDNA and nanosheets, which caused the fluorescence quenching of the tagged fluorophore through FRET. After hybridization of probe and complementary DNA target, the formed double-stranded DNA (dsDNA) weakly interacts with nanosheets due to the shielded nucleobases within the phosphate backbone of dsDNA, which resulted in the low fluorescence quenching of the dye in the presence of nanosheets and provided quantitative detection of target DNA. The quenching property of [Cu(tz)] nanosheets for fluorophore-tagged probe was investigated. Two target ssDNAs (denoted as T1 and T2) were derived from the segment of human P53 tumor suppressor gene. Their fully complementary ssDNAs (denoted as P1 and P2) were respectively labeled with cyanine5 (Cy5) and tetramethylrhodamine (TAMRA), and used as the probes. By adding [Cu(tz)] nanosheets into Cy5-tagged P1 solution, fluorescence of Cy5 was quenched accordingly, and quenching efficiency gradually increased from 35.9% to 96.2% with the increasing concentration of nanosheets from 20 μg/mL to 100 μg/mL (Fig. S5a in Supporting information). Under the optimum concentration (100 μg/mL), the nanosheet possessed fast quenching kinetics, with a high quenching efficiency above 96% after [Cu(tz)] nanosheets were mixed with P1 for 7 min (Fig. 2b), indicating that the P1-adsorbed [Cu(tz)] nanosensor (denoted as P1/[Cu(tz)]) can be constructed fast and facilely. When P1 was hybridized with T1 and formed dsDNA (P1/T1), its fluorescence was largely retained in the presence of [Cu(tz)] nanosheets (Fig. 2b). The large fluorescence intensity ratio of P1 and P1/T1 ($F_{P1/T1}/F_{P1}$ = 24) after adding [Cu(tz)] nanosheets indicated that the nanosheets have much stronger affinity toward ssDNA than dsDNA, which is beneficial for improving the sensitivity to the target (Fig. 2c). In comparison, with addition of 100 μg/mL of [Cu(tz)] crystals, fluorescence intensities of P1 and P1/T1 were only quenched by 23.3% and 9.1%, respectively, corresponding to $F_{P1/T1}/F_{P1}$ = 1.2 (Fig. 2c and Fig. S5b in Supporting information). The $F_{P1/T1}/F_{P1}$ increased 19-fold from bulk materials to nanosheets, indicating an enhancement in the fluorescence quenching ability for nanosheets. The quenching abilities of possible components in nanosheets were measured by the same assay, and the results indicated that the superior quenching efficiency of the ultrathin CP nanosheet mostly comes from its exposed Cu(I) active sites and 2D morphology (see Fig. S6 in Supporting information for detailed analysis).

According to the above intriguing results, the detection bioassay for DNA sensing was established relied on the ultrathin [Cu(tz)] nanosheets. With the increasing concentration of T1, the Cy5 fluorescence intensity of P1 increased accordingly with addition of 100 μg/mL of [Cu(tz)] nanosheets (Fig. 2d). The linear range of the 2D [Cu(tz)] nanosheet-based nanosensor for T1 was from 0.5 nmol/L to 50 nmol/L, with a limit of detection (LOD) of 144 pmol/L (S/N = 3) (Fig. S7 in Supporting information), which is close to those of other well-performed 2D nanosheets [23–26]. Besides high sensitivity, the assay has high selectivity. Replacing targets with a random or single-base mismatched DNA cannot cause distinct increase of fluorescence signal of probes (Fig. S8 in Supporting information). Furthermore, the [Cu(tz)] nanosheet-based sensor can simultaneously detect two target ssDNAs and achieve multiplex analysis (Fig. S9 in Supporting information).

The above *in vitro* results inspired us to further investigate the potential DNA delivery and intracellular sensing properties of [Cu(tz)] nanosheets. Firstly, the cytotoxicity of [Cu(tz)] nanosheets for human lung cancer cell line (A549) was measured

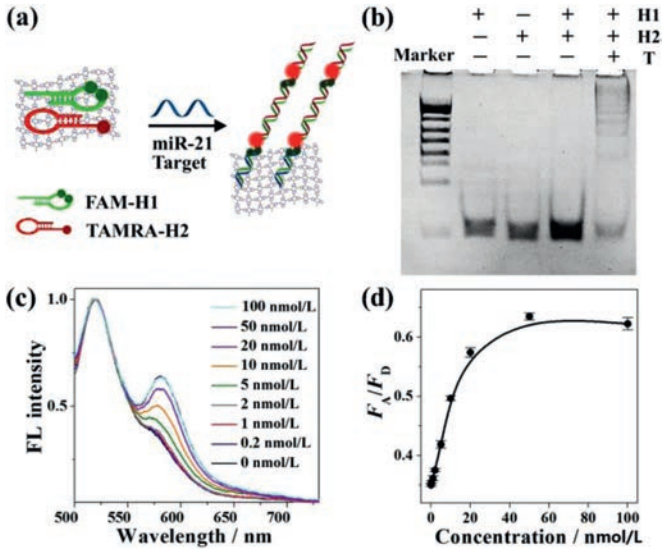

Fig. 3. (a) Schematic illustration of the fluorescence nanosensor based on [Cu(tz)] nanosheet for miR-21 detection with HCR assistance. (b) PAGE image for HCR assay. (c) Fluorescence spectra of HCR/[Cu(tz)] system with different concentrations of miR-21 target after normalized to F_D. (d) The plot of F_A/F_D *vs.* target concentrations.

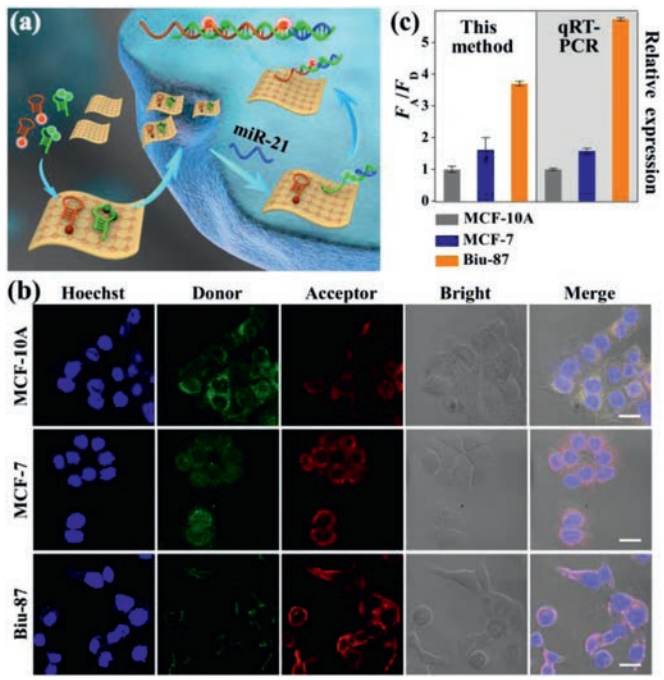

Fig. 4. (a) Schematic illustration of the intracellular delivery of H1 and H2 by [Cu(tz)] nanosheets and intracellular miR-21 sensing. (b) Fluorescence imaging of miR-21 levels by HCR/[Cu(tz)] system in cells including MCF-10A, MCF-7 and Biu-87. Scale bar: 20 μm. (c) The relative F_A/F_D obtained by this method (left panel) and the qRT-PCR analysis of miR-21 (right panel).

by standard 3-(4,5-dimethylthiazole)-2,5-diphenyltetrazolium bromide (MTT) assay (Fig. S10 in Supporting information). After 24 h of incubation of A549 cells with the nanosheets (0−1500 μg/mL), more than 95% of cells survived with nanosheet concentration up to 150 μg/mL, and the IC_{50} value was 352 μg/mL, indicating the low cytotoxicity of the nanosheets. After confirming the low cytotoxicity, the intracellular delivery capacity of [Cu(tz)] nanosheets for ssDNA was then verified by comparing the cellular uptake of P1/[Cu(tz)] and that of free P1 in A549 cells (Fig. S11 in Supporting information). The cells incubated with P1/[Cu(tz)] presented stronger P1 fluorescence comparing to that of free P1, confirming that the nanosheets can deliver ssDNAs into cells. Furthermore, after incubated with T1/[Cu(tz)] for 2 h, the cell imaging of P1 was carried out, of which fluorescence intensity was 60% higher than that of alone P1/[Cu(tz)]-cultured cells. The result suggested that the exogenous ssDNA in living cells can be detected and imaged by the [Cu(tz)]-based nanosensors. Flow cytometry showed that the cell viabilities after each incubation remained above 95% (Fig. S12 in Supporting information), which further demonstrated the low cytotoxity and promising prospect of [Cu(tz)] nanosheets.

As promising diagnostic biomarkers for cancer cells, miRNAs are short (19–22 nucleotides) noncoding RNA. Direct visualization assay of miRNAs in living cells is significant and beneficial for avoiding RNA loss or degradation during RNA extraction [27]. Currently, hybridization chain reaction (HCR)-based FRET strategies have become appealing tools for live-cell miRNA analysis, which usually require nanomaterials to work as nanoquenchers and carriers [28]. Inspired by the appealing DNA delivery and sensing performance, [Cu(tz)] nanosheets were further applied in live-cell miRNA sensing as novel 2D nanocarriers. For proof-of-concept demonstration, miR-21, which is upregulated in many cancer cell lines as an oncogene, was chosen as target. The mechanism of analysis was shown in Fig. 3a. Two hairpin probes (H1 labeled with two FAMs as donors, H2 labeled with one TAMRA as acceptor) [29] are loaded on [Cu(tz)] nanosheets. With addition of miR-21, H1 and H2 will be opened and assembled with each other into dsDNA polymers that left from the nanosheet surface and brought two FAM (donor) groups and one TAMRA (acceptor) group close enough to produce greatly amplified FRET signal.

We testified the self-assembly of the HCR from H1 to H2. The consecutive bands in polyacrylamide gel electrophoresis (PAGE) analysis (Fig. 3b) and the FRET signal in fluorescence spectrum (Fig. S13 in Supporting information) revealed the successful trigger of HCR by the synthetic target miR-21. The efficient quenching of hairpin probes by nanosheets proved the successful construction of hairpin-adsorbed [Cu(tz)] nanosensor (see Fig. S14 in Supporting information for details). To test the *in vitro* sensing feasibility of the HCR/[Cu(tz)] system (H1 + H2 + [Cu(tz)]) toward the target, the kinetics of fluorescence intensity ratio of acceptor and donor (F_A/F_D) was monitored, which gradually increased with prolonged time until 120 min (Fig. S15 in Supporting information). To sensitively detect the low-abundance miRNA, the HCR reaction was prolonged to 4 h, in which the F_A/F_D value enhanced with the increase in target concentration (Figs. 3c and d). The linear range for the detection of miR-21 was from 0.2 nmol/L to 10 nmol/L, with a LOD of 100 pmol/L (S/N = 3). Compared with other widely existed miRNA (let-7a, miR-27a and miR-373), only the target miR-21 can trigger FRET signal (Fig. S16 in Supporting information), demonstrating a high specificity of the HCR/[Cu(tz)] system.

The [Cu(tz)] nanosheet was then utilized to deliver H1/H2 to human breast cancer cell line (MCF-7) for live-cell miRNA sensing (Fig. 4a). Without [Cu(tz)] nanosheets, no fluorescence intensity can be observed after the incubation of MCF-7 cells with free H1 and H2, because of the insufficient cellular uptake of H1 and H2 without carrier (Fig. S17 in Supporting information). Furthermore, negligible red (acceptor) fluorescence signal was observed when H1/[Cu(tz)] or H2/[Cu(tz)] was used to treat the cells separately. Only the cells that were treated with (H1 + H2)/[Cu(tz)] showed obvious green (donor) and red fluorescence signals, suggesting a successful internalization of H1 and H2 by [Cu(tz)] nanosheets and an efficient HCR triggered by the intracellular target miR-21. At the optimized incubation time of 4 h (Fig. S18 in Supporting information), the target sensing of miR-21 in normal and cancer cells was performed (Fig. 4b). Compared to the F_A/F_D of normal

human mammary epithelial cell line (MCF-10A), those for MCF-7 and human bladder cancer cell line (Biu-87) were 1.6-fold and 3.7-fold higher, respectively, which showed the consistent trend with the quantitative reverse-transcription polymerase chain reaction (qRT-PCR) results (Fig. 4c). These results depict a bright future of [Cu(tz)] nanosheets for reliable sensing and imaging of biomolecules in living cells.

In summary, by using a facile surfactant-assisted bottom-up synthesis method, we obtained ultrathin nanosheets (thickness < 5 nm) based on a layered [Cu(tz)] CP. Benefiting from the exposed active sites on 2D planar surface, the obtained [Cu(tz)] nanosheets exhibit drastically improved sensing performances for *in vitro* DNA detection than the bulk form materials. More importantly, owning to the low cytotoxicity and good cellular uptake, the nanosheets can efficiently deliver exogenous DNA probes into living cells. By using an enzyme-free HCR strategy assisted with [Cu(tz)] nanosheets, the reliable detection of miRNA in living cells was realized. These results will facilitate the [Cu(tz)] nanosheet as a novel and promising nanoplatform for biomedical sensing applications. As we evidenced before, the [Cu(tz)] nanosheets can be used as efficient nanocarriers for *in vivo* gene silencing and photodynamic therapy, which encourages us to further explore the possibility of the nanosensor for *in vivo* miRNA detection in the future.

Declaration of competing interest

The authors declare that they have no known competing financial interests or personal relationships that could have appeared to influence the work reported in this paper.

Acknowledgments

This work was supported by the National Key Research and Development Program of China (No. 2018YFA0902801), the National Natural Science Foundations of China (Nos. 21775169, 21801259 and 21974153), the Scientific Technology Project of Shenzhen City (No. JCYJ20200109142410170), the Scientific Technology Project of Guangzhou City (No. 202103000003), the Guangdong Natural Science Foundation (Nos. 2018A030313290, 2019A1515010587), the Guangdong Science and Technology Plan Project (No. 2020B1212060077), and the Fundamental Research Funds for the Central Universities, SYSU (No. 19lgpy142).

Supplementary materials

Supplementary material associated with this article can be found, in the online version, at doi:10.1016/j.cclet.2021.07.041.

References

[1] L. Yang, B. Liu, N. Li, B. Tang, Acta Chim. Sin. 75 (2017) 1047–1060.
[2] J. Yu, S. He, C. Shao, H. Zhao, J. Li, L. Tian, Nanoscale 10 (2018) 7067–7076.
[3] X. Miao, Z. Cheng, H. Ma, et al., Anal. Chem. 90 (2017) 1098–1103.
[4] D. Samanta, S.B. Ebrahimi, C.D. Kusmierz, H.F. Cheng, C.A. Mirkin, J. Am. Chem. Soc. 142 (2020) 13350–13355.
[5] H. Zhang, P. Xu, X. Zhang, et al., Chin. Chem. Lett. 31 (2020) 1083–1086.
[6] W.R. Algar, M. Massey, U.J. Krull, Trac. Trends Anal. Chem. 28 (2009) 292–306.
[7] C. Li, Y. Zhang, J. Chen, et al., Talanta 226 (2021) 122114.
[8] C. Tan, X. Cao, X.J. Wu, et al., Chem. Rev. 117 (2017) 6225–6331.
[9] W. Quan, W. Xudong, X. Min, X. Lou, X. Fan, Chin. Chem. Lett. 30 (2019) 1557–1564.
[10] G.R. Bhimanapati, Z. Lin, V. Meunier, et al., ACS Nano 9 (2015) 11509–11539.
[11] Y. Guo, X. Zhang, F.G. Wu, et al., J. Colloid Interface Sci. 530 (2018) 511–520.
[12] K. Lu, T. Aung, N. Guo, R. Weichselbaum, W. Lin, Adv. Mater. 30 (2018) 1707634.
[13] M. Zhao, Y. Huang, Y. Peng, et al., Chem. Soc. Rev. 47 (2018) 6267–6295.
[14] C. Cui, G. Li, Z. Tang, Chin. Chem. Lett. 32 (2021) 3307–3321.
[15] Y.Z. Li, Z.H. Fu, G. Xu, Coordin. Chem. Rev. 388 (2019) 79–106.
[16] Y. Li, J. Huang, Z.W. Mo, et al., Sci. Bull. 64 (2019) 964–967.
[17] S.C. Junggeburth, L. Diehl, S. Werner, et al., J. Am. Chem. Soc. 135 (2013) 6157–6164.
[18] S.Y. Liu, Y. Xu, H. Yang, et al., Adv. Mater. 33 (2021) 2100849.
[19] A. Gallego, C. Hermosa, O. Castillo, et al., Adv. Mater. 25 (2013) 2141–2146.
[20] J.P. Zhang, Y.Y. Lin, X.C. Huang, X.M. Chen, J. Am. Chem. Soc. 127 (2005) 5495–5506.
[21] S.Y. Liu, D.D. Zhou, C.T. He, et al., Angew. Chem. Int. Ed. 55 (2016) 16021–16025.
[22] C.F. Holder, R.E. Schaak, ACS Nano 13 (2019) 7359–7365.
[23] F. Li, H. Pei, L. Wang, et al., Adv. Funct. Mater. 23 (2013) 4140–4148.
[24] C. Zhu, Z. Zeng, H. Li, et al., J. Am. Chem. Soc. 135 (2013) 5998–6001.
[25] J.M. Fang, F. Leng, X.J. Zhao, X.L. Hu, Y.F. Li, Analyst 139 (2014) 801–806.
[26] S.N. Zhao, L.L. Wu, J. Feng, S.Y. Song, H.J. Zhang, Inorg. Chem. Front. 3 (2016) 376–380.
[27] J. Chen, W. Yin, Y. Ma, et al., Chem. Commun. 54 (2018) 13981–13984.
[28] S. Bi, S.Z. Yue, S.S. Zhang, Chem. Soc. Rev. 46 (2017) 4281–4298.
[29] M. Ou, J. Huang, X. Yang, et al., ChemBioChem 19 (2018) 147–152.